

Critical currents and vortex-unbinding transitions in quench-condensed ultrathin films of bismuth and tin

K. Das Gupta, Swati S. Soman, G. Sambandamurthy,* and N. Chandrasekhar†

Department of Physics, Indian Institute of Science, Bangalore, India

(Received 8 April 2002; published 30 October 2002)

We have investigated the I - V characteristics of strongly disordered ultrathin films of Bi and Sn produced by quench condensation. Our results show that both these systems can be visualized as strongly disordered arrays of Josephson junctions. The experimentally observed I - V characteristics of these films are hysteretic when the injected current is ramped from zero to critical current and back. These are remarkably similar to the hysteretic I - V of an underdamped single junction. We show by computer simulations that hysteresis can persist in a very strongly disordered array. It is also possible to estimate the individual junction parameters (R , C , and I_c) from the experimental I - V of the film using this model. The films studied are in a regime where the Josephson-coupling energy is larger than the charging energy. We find that a simple relation $I_c(T) = I_c(0)[1 - (T/T_c)^4]$ describes the temperature dependence of the critical current quite accurately for films with sheet resistance $\sim 500 \Omega$ or lower. We also find evidence of a vortex-unbinding transition in the I - V taken at temperatures slightly below the mean-field T_c .

DOI: 10.1103/PhysRevB.66.144512

PACS number(s): 74.40.+k, 74.80.Bj, 73.50.-h

I. INTRODUCTION

Ultrathin films produced by quench condensation under highly reproducible conditions, with extensive atomic-scale disorder, have been investigated over the past two decades as model systems to study the interplay between disorder, interactions, and superconductivity. More than a dozen single and multicomponent systems—Al, Bi, Be, Ga, In, Pb, Sn, Nb, Mo-C, Mo-Ge, etc.^{1-9,11}—have been shown to exhibit an insulator-superconductor transition as their thickness is increased or disorder is reduced. The sheet resistance at which the transition takes place has been observed to vary from $\approx 3 \text{ k}\Omega$ in Mo-C films⁹ to $\approx 20 \text{ k}\Omega$ in Al on Ge.¹⁰ The nature of this transition in the $T \rightarrow 0$ limit has attracted maximum attention,^{12,13} with the parameters characterizing the superconducting state having received comparatively lesser attention. It is also unclear at this point what the order parameter of this transition is and what similarities in physics the phenomenon has with metal-insulator transitions in two-dimensional electron gas (2DEG) systems. Most of the reported data on these systems do not show hysteresis in I - V characteristics, the reason being that in most cases they are not probed with currents close to the critical currents of these films. Many physically relevant microstructural parameters can, however, be estimated from the hysteretic I - V .

In this paper we present some experimental results on quench-condensed superconducting films of Bi and Sn. The choice of the two materials was dictated by certain experimental considerations, to be discussed below. Earlier studies had classified materials like Sn, Pb, and Ga as “granular” and Bi (particularly Bi quenched on a thin Ge underlayer) as “homogeneous.” The basis of this classification lay in the rather different resistive transitions to the superconducting state exhibited by these films. In Pb, Ga, and Sn a metallic phase appears to be sandwiched between the insulating and superconducting phases. This observation has stimulated the study of a Bose-metal phase in the $T \rightarrow 0$ limit.¹² It was first

suggested by Ramakrishnan¹⁴ that a “phase-only” picture was appropriate for the granular films. Destruction of superconductivity in these films was thought to take place by destruction of phase coherence (via Josephson coupling) between superconducting grains embedded in a nonsuperconducting matrix. In the homogeneous films (Bi has been taken to be a representative of this class), on the other hand, destruction of superconductivity was thought to take place via destruction of the amplitude of the wave function. Though the resistive transitions (R - T traces) as a function of increasing (decreasing) thickness (disorder) for Bi and Sn show qualitative differences, we show using experimentally obtained I - V characteristics and computer simulations that both these systems can be understood as disordered arrays of Josephson junctions.

Some recent scanning tunneling microscopy (STM) studies^{15,16} on these films suggest that the structure of the first monolayer of atoms that stick to the substrate may be rather different than the subsequent upper layers. Cluster sizes in the range of $\sim 30 \text{ \AA}$ were observed in films nominally 10 monolayers thick. We discuss the relevance of these to the observed properties of our films. The structure of these films remains a mystery. Recent STM data are an indication of what one may expect, but since they were taken under conditions different from experiments such as those of Henning *et al.*,¹⁷ Goldman and co-workers,^{1,5,6} and this work, comparisons of microstructure should be made with an element of caution.

To summarize, there are significant unresolved problems regarding the processes that can lead to formation of such clusters at very low ($< 10 \text{ K}$) substrate temperatures. Landau and co-workers¹⁸⁻²⁰ pointed out that the formation of structures such as those reported by Ekinici and Valles^{15,16} require that incoming atoms be able to perform ~ 500 hops before they finally settle to their positions. This order of diffusivity is much more than what incoming atoms striking cold substrates are believed to have, although such a possibility can-

not be ruled out. We have not addressed this question, but show that several properties of the superconducting state in these films may be understood if we accept the presence of superconducting and nonsuperconducting regions in close proximity in the film, a case of microstructure similar to that reported by Ekin and Valles.^{15,16} Our model bears a close resemblance to the “percolation-type” model used by Meir²¹ in describing the $M-I$ transition in 2DEG and has been discussed in our earlier work.³

II. EXPERIMENTAL SETUP

The experiments were done in a UHV cryostat, custom designed for *in situ* study of ultrathin films, described in our earlier publications.^{2,3} A turbomolecular pump, backed by an oil-free diaphragm pump, provided a vacuum better than 10^{-8} Torr. The substrate was either *a*-quartz or crystalline sapphire, mounted with adequate thermal contact on a copper cold finger, in contact with a pumped helium bath. The lowest attainable temperature was 1.8 K. The material (e.g., Bi, Sn) was evaporated from a pyrolytic boron nitride crucible in a Knudsen cell (effusion cell) of the type used in molecular beam epitaxy (MBE). The temperature of the cell was carefully controlled to give a steady deposition rate between 1 and 5 Å/min. The required temperatures were 650 °C for Bi and 1150 °C for Sn.

Two Hall-bar type masks defined the sample; the actual sample size was 6 mm×1 mm. One of the samples had a predeposited Ge underlayer of ≈ 10 Å thickness. This geometry enables us to evaluate the claim that Ge underlayers may significantly improve the wetting properties of the films and the possibility that there may be screening effects due to the presence of an underlayer of a dielectric constant larger than that of the substrate. The metal flux reached the sample through carefully aligned holes in successive cryoshields cooled by liquid helium and nitrogen. These shields also reduce the heat load on the sample and provide cryopumping, for better vacuum in the neighborhood of the sample. Electrical contacts to the films were provided through predeposited platinum contact pads, about 50 Å thick. Four-probe dc measurements were carried out using a standard high-impedance current source and a nanovoltmeter or an electrometer.

III. OBSERVATIONS AND DISCUSSION

The $R-T$ traces of a series of Sn films exhibiting the $I-S$ transition are shown in Fig. 1. Figure 2 shows a typical set of observed $I-V$ characteristics for a Bi film in the superconducting regime. We can read off the critical and retrapping currents for the whole film. We claim here (and demonstrate later) that this ratio would be nearly same as that of a single junction. For a single junction we have the exact relation between the Josephson coupling energy, charging energy, normal-state resistance, and the Stewart-McCumber junction parameter β :

$$E_J/E_c = (2/\pi^2)(R_Q/R_N)^2\beta, \quad (1)$$

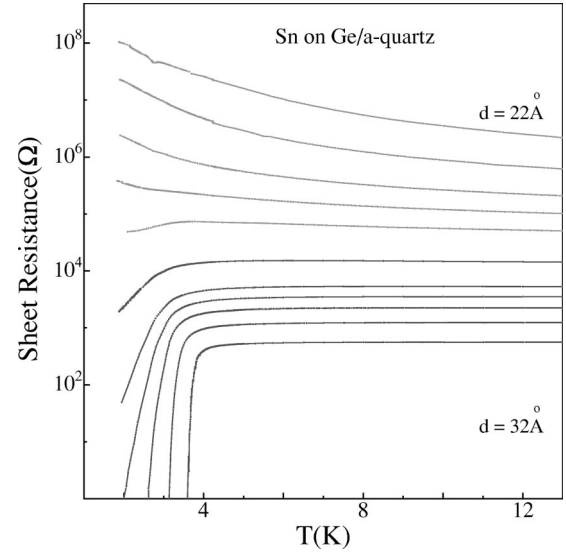


FIG. 1. Resistance-temperature ($R-T$) curves of a set of quench-condensed Sn films showing the insulator-superconductor transition.

where $R_Q = h/4e^2$. With the approximations stated above, for a film with $R_{\square} \approx 500 \Omega$ and $\beta \approx 2$, we get $E_J/E_c \approx 70$. This places the films for which we find a simple empirical relation between the critical current and temperature, well into the regime $E_J \gg E_c$.

The $I-V$ characteristics of a single Josephson junction (JJ), in the framework of the RCSJ model, is well known and is discussed in several texts.²² If the transfer of a Cooper pair across the junction causes negligible change in the phase difference (ϕ) across the junction, then ϕ can be viewed as a continuous variable and the $I-V$ characteristics (neglecting the effect of thermal noise) can be deduced from Eq. (2):

$$\beta\dot{\phi} + \phi + \sin \phi = i. \quad (2)$$

The long-time average $\langle \dot{\phi} \rangle$ gives the observed voltage drop. i is the normalized current, I/I_c , through the junction. β is

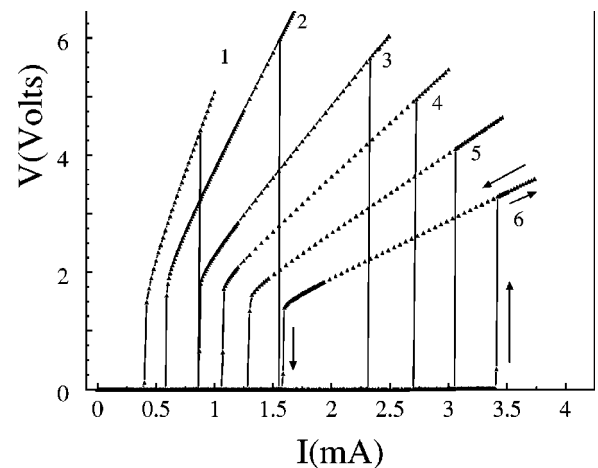


FIG. 2. Current-voltage ($I-V$) characteristics of Bi films on sapphire. The observed characteristics are similar for Bi and Sn on crystalline as well as amorphous substrates.

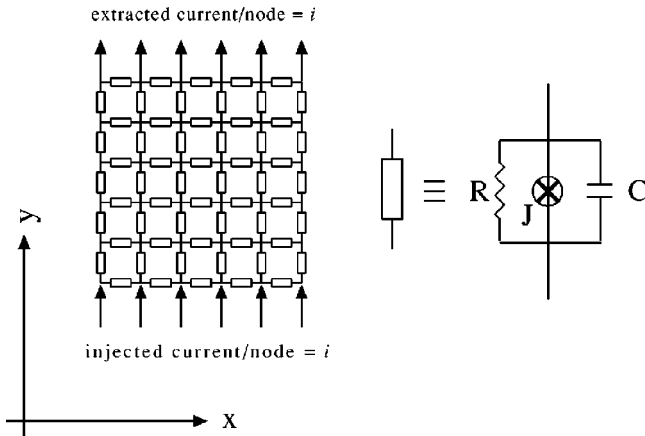


FIG. 3. Schematic of a 5×5 JJ array. Each bond is a parallel combination of three elements, as shown. The current is injected and extracted as shown; in the other direction we use periodic boundary condition.

related to the microscopic parameters of the junction as $\beta = (2eI_c R_N / \hbar) R_N C$ and also fixes the ratio of the retrapping to critical currents (I_r / I_c). The larger the value of β , smaller is this ratio and wider the hysteresis.

We first investigate, by computer simulations, whether the hysteresis would persist in a 2D RCSJ array even if all the junction parameters are allowed to have a large distribution of values (i.e., in presence of strong disorder). Also we need to know whether the observed I - V curve would be significantly altered by the particular type of distribution (e.g., square, Gaussian, log-normal). We address these questions in the section on computer simulation, the details of which are presented later.

An important fact about a 2D network of resistances is the following: not too close to the percolation threshold, the observed resistance, measured between two edges (see Fig. 3), is close to the average value of all the resistances. In a 1D chain it is obviously the sum of all the resistances, in a 3D lattice the measured resistance is much lower than the average. These can be verified by simple numerical calculations. In 2D even when the width of the distribution is more than 90% of the mean value, the measured normal-state sheet resistance (R_{\square}) of the film does not differ from the mean of all the resistances by more than 10%. We have verified by direct numerical calculation that this result holds good for array sizes down to a 10×10 array. If there are N junctions in parallel, then the observed critical current of the array would be approximately N times the average critical current of one junction. This allows us to infer some important facts. This also demonstrates our claim above that the ratio of the critical current to the retrapping current for an array is the same as that for a single junction in the array. In what follows, this will be further substantiated.

A. Hysteresis in a disordered array

If identical junctions were laid out on an array, the I - V characteristics would be indistinguishable from that of a single junction in absence of a magnetic field. However,

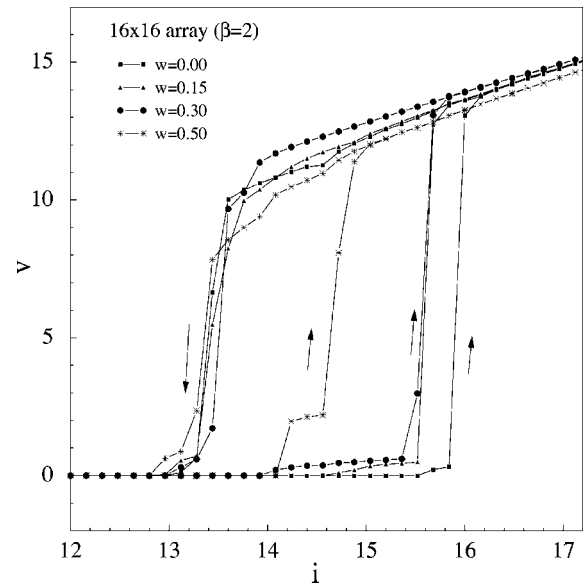


FIG. 4. Computer-simulated I - V curves of a 16×16 array of Josephson junctions, on a square lattice. The bond parameters (R, C, I_c) are chosen from a square distribution—“ w ” denotes the width of the distribution as a fraction of the mean value of the parameters. The mean values are used to calculate β . Use of a “log-normal” distribution also leads to similar results.

when there is a large spread in the values of the junction parameters, it is not *a priori* obvious what their behavior will be. This is because different junctions with different critical currents may undergo transitions at different currents, and for a large array the sharp transition might be broken into many steps and then rounded off by finite-temperature effects. Our main result in this regard is that, even in a small array (16×16), disorder does not completely destroy the hysteresis—until about 50% disorder (ratio of width to mean value in a square distribution) the shape of the I - V loop does not change appreciably. We have shown the results (see Fig. 4), using a square distribution of disorder here, though simulations using a log-normal distribution (results not shown) also lead to similar conclusion.

1. Driving equations and the algorithm

In an array the algebraic sum of all the currents meeting at any node must be zero—this is required by Kirchoff’s current law. As shown in Fig. 3, the current is fed uniformly through one edge of the array and extracted through the opposite. In the direction perpendicular to that of current injection, we generally use periodic boundary conditions; this is equivalent to joining the remaining two free edges of the array together. From the current conservation equations we get a total of N^2 coupled second-order differential equations. The model we are considering neglects the self-inductance of the array. Consider a single node (not on any of the edges), at which the phase at some instant is ϕ . In the four neighboring nodes the phases are $\phi_u, \phi_l, \phi_b, \phi_r$ —where the subscripts denote up, left, bottom, and right, respectively. Every bond will have its characteristic R, C , and I_c value—since the array is disordered. We use R_0, C_0 , and I_{C0} to denote the

average values. With a little algebra we can show that the contribution of any link to a node is

$$i = c\beta_0\dot{\phi} + r\dot{\phi} + i \sin \phi,$$

where, for a completely ordered array $r=1$, $c=1$ for all bonds. Adding all the current contributions to a node we get

$$\begin{aligned} \beta_0[(c_l + c_u + c_r + c_b)\dot{p} - c_l\dot{p}_l - c_u\dot{p}_u - c_r\dot{p}_r - c_b\dot{p}_b] \\ + (1/r_l + 1/r_u + 1/r_r + 1/r_b)p - (p_l/r_l + p_u/r_u \\ + p_r/r_r + p_b/r_b) + (i_l s_l + i_u s_u + i_r s_r + i_b s_b) = 0, \end{aligned} \quad (3)$$

where $\dot{\phi}_{l,u,r,b} = p_{l,u,r,b}$ and $\sin(\phi - \phi_{l,u,r,b}) = s_{l,u,r,b}$. For the nodes on the boundary, there will be three contributions from the three nearest neighbors; the fourth contribution will be $\pm i$, depending on whether current is injected or extracted from the node. Thus we get a total of N^2 coupled second-order differential equations, where (p, ϕ) form a total of $2N^2$ variables to be updated at each step. We can visualize the whole set of equations, in a matrix form, as

$$\begin{aligned} \mathbf{C}\dot{\mathbf{P}} &= \mathbf{R}\mathbf{P} + \mathbf{I}\mathbf{S} = \mathbf{D}, \\ \dot{\mathbf{\Phi}} &= \mathbf{P}, \end{aligned} \quad (4)$$

where \mathbf{P} , \mathbf{D} , \mathbf{S} , and $\mathbf{\Phi}$ are column vectors of length N^2 each, and \mathbf{C} , \mathbf{R} , and \mathbf{I} are $N^2 \times N^2$ matrices. These matrices do not change with time. However, \mathbf{C} is a singular matrix, irrespective of whether the array is regular or disordered. This singularity implies that all the variables in the problem are not independent. This introduces an extra complication in the problem. In the mathematical literature such systems of equations are called ‘‘differential algebraic equations’’ (DAE’s). They occur frequently in lattice-related problems.

Physically it is not difficult to trace the equation of constraint here. We have written equations for the phase of each junction, whereas only the phase differences are of consequence. We can add an arbitrary number to each phase ensuring

$$\sum_{\text{all nodes}} \phi_i = 0.$$

This is achieved by setting all the numbers in any row (say, the last) of the matrix \mathbf{C} to be equal to 1 and the corresponding entry in the column vector \mathbf{D} to be 0. The modified \mathbf{C} is no longer singular and can be inverted. The set of equations is solved by using a fourth-order Runge-Kutta method with variable time stepping.²³

For each current we allow the system to evolve until $\tau = 2500$; the first 500 time units are regarded as stabilization time and discarded. The voltage across the array is then averaged between $500 < \tau < 2500$. The value of the external current is then increased by a small amount and the above-mentioned cycle repeated, until the injected current reaches the desired maximum value. After that it is decremented in identical steps. The recorded values of the voltage vs drive

current are the response of the array to a cyclic external current. The I - V curve obtained this way is hysteretic for $\beta_0 > 1$, as expected.

In this algorithm every step requires a large ($N^2 \times N^2$) matrix multiplication. This requires N^4 multiplications for each update of the variables. Assuming that in each step we change the current fed to the array by I_C/N , where I_C is the average critical current of each bond, the total complexity of the simulation increases as $\sim N^5$.

2. ‘‘Fast’’ algorithm for regular arrays

For ordered arrays the computation can be made much faster, exploiting the special form the matrix \mathbf{C} takes in such a case. The matrix \mathbf{C} is then a ‘‘connectivity matrix’’; the (\vec{r}, \vec{r}') element of the matrix will be -1 if the sites \vec{r} and \vec{r}' are connected by a bond, and the diagonal element will give the coordination number of the site. Himbergen *et al.*²⁴ noted that this particular form of the matrix allows the multiplication to be carried out in $\sim N \ln N$ steps. Because the eigenvectors of this matrix are of the form $\exp(i\vec{k} \cdot \vec{r})$, the multiplication with the inverse of the matrix can be viewed as two discrete Fourier transforms, amenable to ‘‘fast Fourier transform’’ techniques. The technique was improved by Dominguez *et al.*²⁵ and applied to several array geometries soon after.²⁶ Unfortunately, this fast algorithm requires that the capacitance of all the bonds be same, even though disorder in R and I_C can be handled. We however need to see the effect of disorder in all the bond parameters. Consequently we had to use straightforward matrix multiplication—i.e., the ‘‘slow’’ technique.

B. Critical currents of the films

We next investigate the temperature dependence of the experimentally measured critical currents. Here we plot the normalized critical current against the reduced temperature. Figure 5 shows data from several Bi films, gathered from different runs and on different substrates. All the points appear to collapse on a simple power law curve, given by

$$I_c(T)/I_c(0) = 1 - (T/T_c)^4. \quad (5)$$

A similar behavior of Sn films is also shown in Fig. 5. The critical current of a weak link is related to the superconducting gap (Δ) by the well-known Ambegaokar-Baratoff relation

$$I_c R_N = (\pi \Delta(T)/2e) \tanh \Delta(T)/(2k_B T). \quad (6)$$

As $T \rightarrow T_c$, $\Delta \rightarrow 0$, we can expand the \tanh term to show that $I_c \sim \Delta^2$. This suggests that for these films Δ vanishes as $\sqrt{1 - (T/T_c)^4}$. Near T_c , we have $\sqrt{1 - (T/T_c)^4} \approx 2\sqrt{1 - (T/T_c)}$, which is consistent with the behavior of a BCS gap, as far as the leading power is concerned. However, inserting the BCS result, [i.e., $\Delta(T)/\Delta(0) \approx 1.74\sqrt{1 - T/T_c}$] in the Ambegaokar-Baratoff relation leads to the well-known prediction that near T_c , the slope [$I_c R_N/(T - T_c)$] should be $635 \mu\text{V/K}$. For all the Bi and Sn films studied by us, we found this slope to be $960 \pm 20 \mu\text{V/K}$.

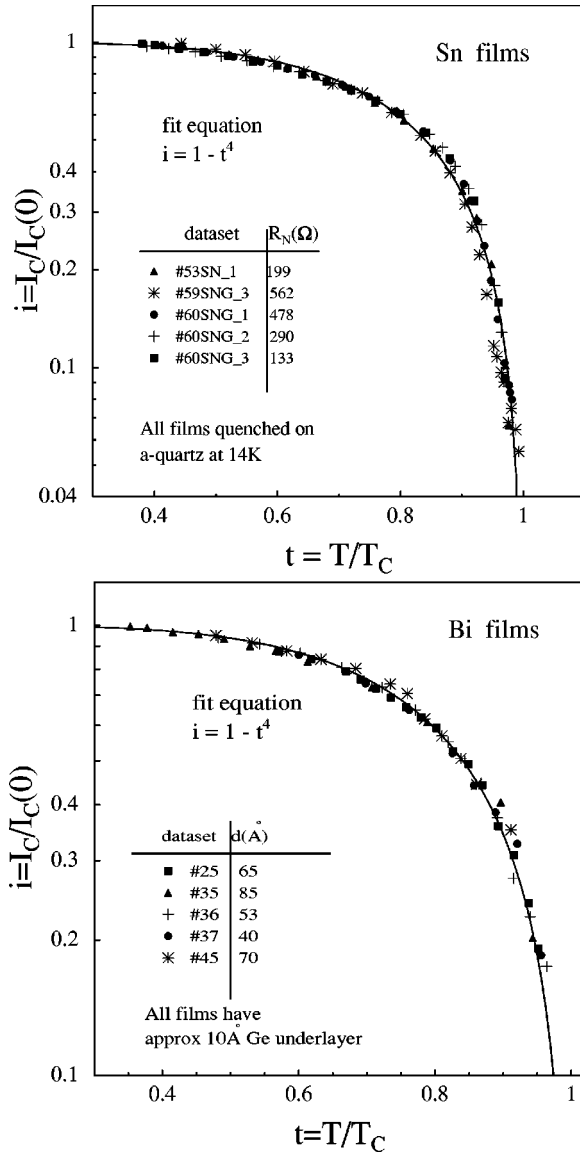


FIG. 5. Critical currents of a set of Bi and Sn films of low sheet resistance, in the regime $E_J \gg E_c$. Both show a similar power-law behavior over the entire temperature range.

It is interesting to note here that a similar behavior of $\Delta(T)$ [i.e., $\sim \sqrt{1 - (T/T_c)^4}$] over the entire range of temperature has been observed in fabricated Josephson junction arrays.²⁷ In such fabricated arrays, one naturally expects the spread of the junction parameters to be quite narrow, and in this sense the disorder is considerably less than that for a random array, such as the quench condensed films we study in this work.

Though the data sets are restricted to $T/T_c > 0.3$, in all the experiments, the flattening of the curves allows us to make an extrapolation of the critical current to the $T \rightarrow 0$ limit. This is important, since $I_c(0)$ is very simply related to the superconducting gap by Eq. (6). This relation can be refined further to account for the presence of disorder, as has been done by Kulik and Omel'yanchuk.²⁸ In fact, disordered films may show a much better match to the Kulik-Omel'yanchuk form, rather than the Ambegaokar-Baratoff form. Since the Kulik-

TABLE I. The estimates of the number of junctions for Bi films. This estimate is for a 1 mm \times 1 mm area.

Data set	Thickness	T_c (K)	$R_N(\Omega)$	N	$4I_c(0)R_N/T_c$
No. 36	53 Å Bi	4.32	421	942	953
No. 25	65 Å Bi/Ge	4.5	236	651	954
	65 Å Bi	4.29	252	730	955
No. 35	85 Å Bi/Ge	5.23	135	473	954

Omel'yanchuk form comprises recursive functions, no simple expression exists for the dependence of the gap or critical current on reduced temperature.²⁸ However, the corrections for the presence of disorder to the Ambegaokar-Baratoff relation, near $T=0$, are within a factor of 2 for both the dirty and clean limits. This increase for the dirty limit may partly explain the reason for the steeper dependence of i on t observed in this work. Very close to T_c it coincides with Eq. (6).

As an interesting aside, we mention that Dynes *et al.* have shown in tunneling experiments on quenched Sn and Pb films²⁹ that the ratio $2\Delta(0)/k_B T_c$ remains close to 3.5 (the BCS value) for sheet resistances upto at least 4 k Ω . The agreement was better for Sn than Pb; this may be expected as Pb is a "strong-coupling" superconductor.

C. Estimate of the number of junctions in a film

Using the model of the disordered array as the background and the extrapolated values of the critical current at $T=0$, we show that an estimate of the number of junctions in the film can be made. The estimate shows that not all grain boundaries may be acting as junctions or weak links. It also supports the possibility that the first layer of atoms that stick to the substrate may have a significantly different structure^{15,16} than the subsequent upper layers. In such cases a slightly more uniform lower layer may offset the phase-breaking effect of a considerable number of grain boundaries.

If superconducting behavior of each grain follows approximately the BCS model, then we should have the zero-temperature gap $\Delta(0) = 1.76k_B T_c$. Such an assumption is certainly valid in the vicinity of T_c , deviations from this being important only at lower temperatures, as discussed above. The average critical current of each junction is I_c/N , where I_c and T_c are experimentally measured. The number of junctions acting in parallel should then be given by

$$I_c R_N / N = \pi \Delta(0) / 2e = \pi (1.76k_B T_c) / 2e. \quad (7)$$

The total number of junctions (over 1 mm \times 1 mm) is then approximately N^2 . Using the critical current data shown and their T_c we find the Bi films the parameters given in Table I.

We find that there are $\sim 10^6$ junctions/mm² in a ≈ 60 Å film. As expected the number of junctions reduce when the film thickness is increased. This is expected as many of the gaps and voids between grains may be filling up as more material is deposited, reducing the number of junctions.

Based on this we obtain the following values for ω , R , and C for the 85 Å film at $T=0$:

$$\beta = 4.5, \quad \omega = 3.63 \times 10^{12} \text{ rad/sec}, \quad I_c/\text{bond} = 8.9 \text{ } \mu\text{A}, \quad C_{\text{bond}} = 9 \times 10^{-15} \text{ F},$$

which are reasonable values.

We find that at low temperatures I_c tends to a constant value and so does I_r . This implies that the ratio I_r/I_c and hence β also varies very little at low temperatures, which is to be expected. Near T_c the behavior is dominated by the variation of the critical current of the bond. The values of the capacitance and resistance (normal state) do not vary much with temperature. We also find that for this value of thickness, the film is in a regime where the charging energy and ‘‘Coulomb blockade’’ are negligible compared to the Josephson-coupling energy at low temperatures. The value of the capacitance will, however, reduce drastically if the thickness of the film is lesser. In fact a recent optical frequency measurement¹⁷ of the intergrain capacitance, in much thinner Pb films, reported a value of $\sim 2 \times 10^{-19}$ F, which can be compared with the values we have inferred above. In such cases single-electron tunneling effects may be expected to play a very important role in transport processes. It is interesting to compare the values we have estimated with typical values of ‘‘fabricated’’ regular Josephson-junction arrays. From the published literature we pick one work²⁷ we have already cited earlier. We find that the arrays used had a typical junction capacitance of $1-3 \times 10^{-15}$ F, junction area of $\sim 1 \text{ } \mu\text{m}^2$, and junction resistance of 4–150 k Ω . These values, particularly those of the junction capacitance and ‘‘unit cell’’ area that we have estimated, are of the same order. However, the values of Josephson-coupling energy (and hence I_c/bond) reported by them are much less compared to deposited films. Thus the screening effects of the supercurrents flowing in the films may be expected to be much greater than in fabricated arrays. The current density would surely have a lot of spatial variation—if, however, we deliberately neglect this aspect and calculate a supercurrent density a film (taking the nominal thickness to be the average thickness) can support before going normal; for the 85 Å film we get a number $\sim 10^5$ A/cm², which can be compared with typical values reported for disordered films of the copper oxide superconductors.

D. Possible Kosterlitz-Thouless transition in presence of strong disorder

In an ordered array of Josephson junctions, at finite temperatures vortex-antivortex pairs are generated spontaneously. These vortices may be visualized as a circulating pattern of the ‘‘phase variable’’ in neighboring islands, several characteristics of these vortices have been studied in superfluids and arrays. One of the atomic scale disordered systems that has been studied with respect to the Kosterlitz-Thouless (KT) transition is the quenched Hg-Xe mixture.³⁰ In this section we investigate whether some of the observed characteristics of the I - V curves of disordered Sn and Bi films can be attributed to a Kosterlitz-Thouless-type transition.

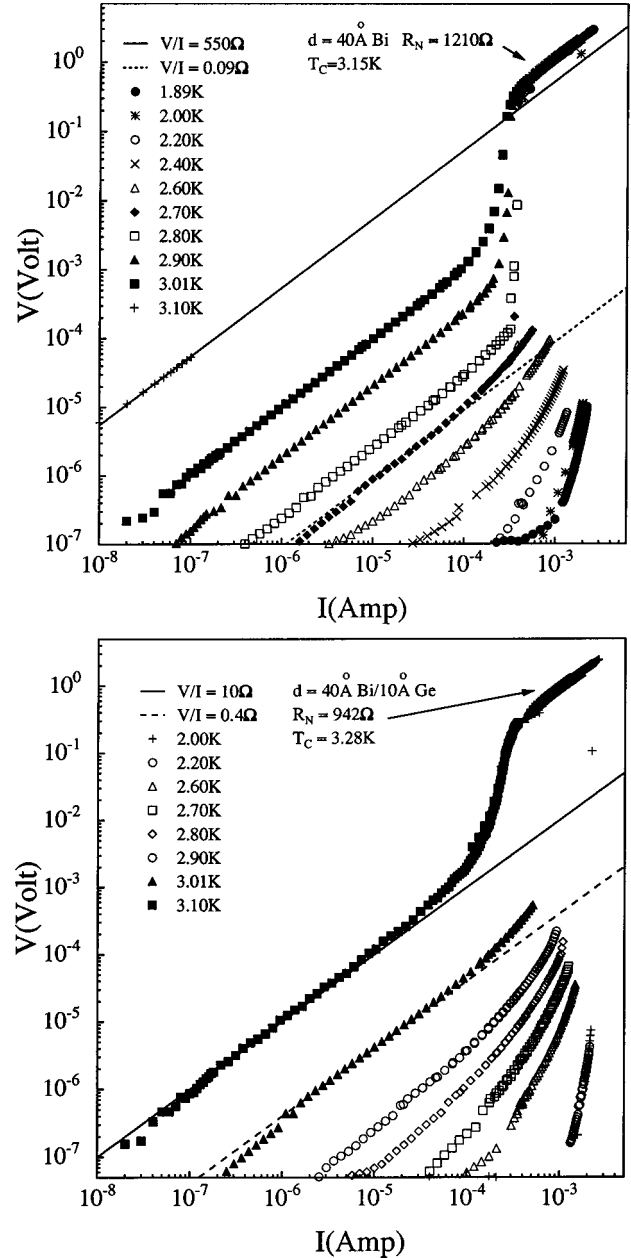


FIG. 6. Data from a 40 Å film on bare quartz (upper panel) and with 10 Å Ge underlayer (lower panel). Although the I - V are hysteretic, the hysteresis is not shown for purposes of clarity. In both cases, a few I - V curves below T_c have a linear part. Data taken at lower temperatures do not show a power-law behavior (linear region in a log-log plot).

Figure 6 shows a set of I - V curves taken at various temperatures. All the curves show a clear critical current and retrapping current—and a transition to the normal-state resistance of 1210 and 942 Ω for this particular film. For a few temperatures just below T_c , the ‘‘superconducting state’’ shows dissipation. The resistance remains constant over three to four decades of current and hence there is no self-heating effect. It is tempting to identify the appearance of an Ohmic dissipative state with the unbinding of vortices—the ‘‘Kosterlitz-Thouless’’ transition. However, we need to be cautious with such an identification. One of the signatures of

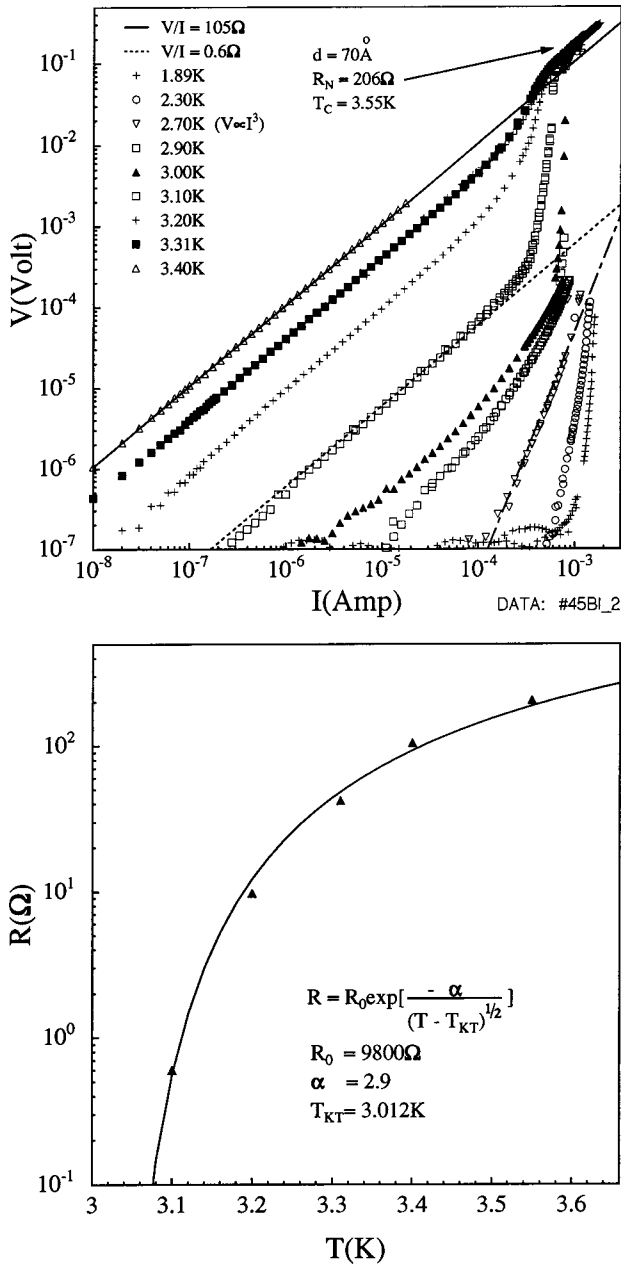


FIG. 7. Data from a 70 Å Bi film shows power-law region in logarithmic plot (upper panel) as well as the predicted dependence of R on T (lower panel). Both of these features together identify a KT transition. Hysteresis is not shown for the sake of clarity.

KT transition is that, below T_{KT} there is a regime where the voltage increases as the cube of the current. The reason for this is that below T_{KT} all the free vortices are generated by the current itself. The current exerts oppositely directed “Lorentz force” on the vortex and the antivortex—and hence tends to create free vortices by breaking the pairs. The number of vortices just below T_{KT} increases as I^2 and hence the voltage rises approximately as I^3 . Even though we may see such linear regions in a logarithmic plot, we do not always find this predicted cubic dependence in that region of temperature. Experiments on proximity coupled arrays³¹ have shown both the linear regime in a logarithmic plot and cubic dependence of voltage on current. In our case we find that

the 70 Å Bi film data show this feature—see Fig. 7 (upper panel)—whereas for many other thicknesses the I - V curves below the possible T_{KT} do not have any region where a $V \propto I^3$ dependence is obvious. Any such behavior should have shown up clearly in a log-log plot. The 70 Å film also shows another characteristic signature of KT transition (lower panel). Above T_{KT} the resistance rises with temperature as

$$R(T) = R_0 \exp[-\alpha/\sqrt{T - T_{KT}}].$$

The “best fit” is shown in Fig. 7. We have a mean-field $T_c = 3.55$ K and $T_{KT} = 3.01$ K for this film. With increasing thickness, the resistive transition becomes steeper and the range of temperature over which the KT-type behavior may be seen also narrows down. For a 100 Å Bi film ($R_{\square} = 106 \Omega$, data not shown) we found that the region narrows down to less than 100 mK. This is to be expected since the thicker films approach 3D behavior and the KT transition is restricted to 2D systems. An important aspect that remains unaddressed is the robustness of the KT transition to disorder. However, since vortices are macroscopic objects, which average over large areas of the films—compared to microscopic atomic-scale disorder—the KT transition may be expected to remain quite robust in presence of disorder.

IV. CONCLUSION

We have shown that several properties of quench condensed films of Sn and Bi can be understood by visualizing them as strongly disordered arrays of Josephson junctions. Superconductor-insulator transitions in such arrays are well known and predicted to occur around $E_j \approx E_c$.^{32,33} Referring to Eq. (2) we can see that it should occur in the vicinity of $R_N \approx R_Q$ but not necessarily exactly at $R_N = R_Q$. A simple power-law behavior of the critical current of these films (with $R_{\square} < 500 \Omega$) is found, and the observed I - V characteristics indicate a possible vortex-unbinding transition in these films. The picture of Josephson coupling between superconducting patches in the film implies that there is a strong variation of carrier density in the film itself. This bears a strong resemblance to the percolation-type description of 2DEG (Ref. 21) that has been successfully used to describe some aspects of the observed metal-insulator transition in Si metal-oxide-semiconductor field-effect transistors (MOSFET’s). To some extent computer simulations can reproduce the behavior of the actual films. The difficulties in doing numerical work on strongly disordered systems are well known. Though a renormalization group analysis of the KT transition has been done,³⁰ the effect of strong screening (i.e., large self-inductance) in a disordered array remains to be investigated.

ACKNOWLEDGMENTS

This work was supported by DST and UGC, Government of India. K.D.G. thanks CSIR, Government of India, for support. We acknowledge discussions with Professor A. M. Goldman and Professor C. J. Adkins.

- *Present address: Department of Condensed Matter Physics, Weizmann Institute of Science, Rehovot, Israel.
- †Electronic address: chandra@physics.iisc.ernet.in
- ¹D.B. Haviland, Y. Liu, and A.M. Goldman, *Phys. Rev. Lett.* **62**, 2180 (1989).
 - ²G. Sambandamurthy, K. Das Gupta, V.H.S. Murthy, and N. Chandrasekhar, *Solid State Commun.* **115**, 427 (2000).
 - ³K. Das Gupta, G. Sambandamurthy, Swati S. Soman, and N. Chandrasekhar, *Phys. Rev. B* **63**, 104502 (2001).
 - ⁴E. Bielejec, J. Ruan, and Wenhao Wu, *Phys. Rev. Lett.* **87**, 036801 (2001).
 - ⁵H.M. Jaeger, D.B. Haviland, B.G. Orr, and A.M. Goldman, *Phys. Rev. B* **40**, 182 (1989).
 - ⁶B.G. Orr, H.M. Jaeger, and A.M. Goldman, *Phys. Rev. Lett.* **53**, 2046 (1984).
 - ⁷B.G. Orr, H.M. Jaeger, and A.M. Goldman, *Phys. Rev. B* **32**, 7586 (1985).
 - ⁸N. Nishida, S. Okuma, and A. Asamitsu, *Physica B* **169**, 478 (1991).
 - ⁹S.J. Lee and J.B. Ketterson, *Phys. Rev. Lett.* **64**, 3078 (1990).
 - ¹⁰Y. Liu and A.M. Goldman, *Mod. Phys. Lett. B* **8**, 277 (1994).
 - ¹¹D. Ephron, A. Yazdani, A. Kapitulnik, and M.R. Beasley, *Phys. Rev. Lett.* **76**, 1529 (1996).
 - ¹²D. Das and S. Doniach, *Phys. Rev. B* **60**, 1261 (1999).
 - ¹³P. Phillips and D. Dalidovich, *Phys. Rev. B* **65**, 081101 (2002).
 - ¹⁴T.V. Ramakrishnan, *Phys. Scr.* **T27**, 24 (1989).
 - ¹⁵K.L. Ekinci and J.M. Valles, Jr., *Phys. Rev. B* **58**, 7347 (1998).
 - ¹⁶K.L. Ekinci and J.M. Valles, Jr., *Phys. Rev. Lett.* **82**, 1518 (1999).
 - ¹⁷P.F. Henning, C.C. Homes, S. Maslov, G.L. Carr, D.N. Basov, B. Nikolić, and M. Strongin, *Phys. Rev. Lett.* **83**, 4880 (1999).
 - ¹⁸A.V. Danilov, S.E. Kubatkin, I.L. Landau, and L. Rinderer, *J. Low Temp. Phys.* **103**, 35 (1996).
 - ¹⁹I.A. Parshin, I.L. Landau, and L. Rinderer, *Phys. Rev. B* **54**, 1308 (1996).
 - ²⁰I.L. Landau, I.A. Parshin, and L. Rinderer, *J. Low Temp. Phys.* **108**, 305 (1997).
 - ²¹Y. Meir, *Phys. Rev. Lett.* **83**, 3506 (1999).
 - ²²M. Tinkham, *Introduction to Superconductivity* (McGraw-Hill, New York, 1996).
 - ²³W.H. Press, S.A. Teukolsky, W.T. Vetterling, and B.P. Flannery, *Numerical Recipes in C* (Cambridge University Press, Cambridge, England, 1993), Chap. 16.
 - ²⁴H. Eikmans and J.E. van Himbergen, *Phys. Rev. B* **41**, 8927 (1990).
 - ²⁵D. Dominguez, J.V. Jose, A. Karma, and C. Weiko, *Phys. Rev. Lett.* **67**, 2367 (1991).
 - ²⁶S. Datta, S. Das, D. Sahadev, R. Mehrotra, and S. Shenoy, *Phys. Rev. B* **54**, 3545 (1996).
 - ²⁷P. Delsing, C.D. Chen, D.B. Haviland, Y. Harada, and T. Cleason, *Phys. Rev. B* **50**, 3959 (1994).
 - ²⁸I.O. Kulik and A.N. Omel'yanchuk, *JETP Lett.* **21**, 96 (1976).
 - ²⁹J.M. Valles, Jr., R.C. Dynes, and J.P. Garno, *Phys. Rev. B* **40**, 6680 (1989).
 - ³⁰A.M. Kadin, K. Epstein, and A.M. Goldman, *Phys. Rev. B* **27**, 6691 (1983).
 - ³¹D.J. Resnick, J.C. Garland, J.T. Boyd, S. Shoemaker, and R.S. Newrock, *Phys. Rev. Lett.* **47**, 1542 (1981).
 - ³²L.J. Geerligs, M. Peters, L.E.M. de Groot, A. Verbruggen, and J.E. Mooij, *Phys. Rev. Lett.* **63**, 326 (1989).
 - ³³W. Zwerger, in *Quantum Coherence in Mesoscopic Systems*, edited by B. Kramer (Plenum Press, New York, 1991).